

Crustal deformation measurements in Guerrero, Mexico

Kristine M. Larson,¹ A. R. Lowry,² Vladimir Kostoglodov,³ Wallis Hutton,⁴ Osvaldo Sánchez,³ Ken Hudnut,⁵ and Gerardo Suárez³

Received 13 October 2003; revised 24 February 2004; accepted 19 March 2004; published 28 April 2004.

[1] GPS measurements of crustal deformation in Guerrero, southern Mexico, include surveys collected between 1992 and 2001 as well as continuous GPS measurements at a few sites. These geodetic observations are used to calculate interseismic deformation rates and assess the presence and possible location of transient deformation during the period encompassing 1992.25 to 2001.75. The data are used to examine transient deformation in 1998 previously described from data at a single site by *Lowry et al.* [2001]. Survey measurements and continuous data from a site near Popocatepetl volcano confirm the 1998 transient, and survey data also suggest another transient occurred following the 14 September 1995 ($M_w = 7.3$) Copala earthquake. All of the available GPS position estimates have been inverted for a combined model of slip during each event plus the steady state slip on the plate interface. Modeling of the steady state deformation rates confirms that the Guerrero seismic gap is partially frictionally locked at depths shallower than about 25 km and accumulating strain that may eventually be released in a great earthquake. The data also suggest that there is frictional coupling to much greater (>40 km) depths, which releases more frequently in aseismic slip events. The locations and sizes of the transient events are only partially constrained by the available data. However, the transient models which best fit the GPS coordinate time series suggest that aseismic slip was centered downdip of the seismogenic portion of the plate-bounding thrust in both events, and the moment release had equivalent magnitudes $M_w = 7.1 + 1.3/-1.0$ in 1995–1996 and $7.1 + 0.4/-0.1$ in 1998. **INDEX TERMS:** 1208 Geodesy and Gravity: Crustal movements—intraplate (8110); 1243 Geodesy and Gravity: Space geodetic surveys; **KEYWORDS:** transient deformation, GPS, Guerrero

Citation: Larson, K. M., A. R. Lowry, V. Kostoglodov, W. Hutton, O. Sánchez, K. Hudnut, and G. Suárez (2004), Crustal deformation measurements in Guerrero, Mexico, *J. Geophys. Res.*, 109, B04409, doi:10.1029/2003JB002843.

1. Introduction

[2] Accurate assessment of the earthquake hazard posed by major faults requires measurements of both interseismic strain accumulation and seismic strain release. The increasing abundance of continuous GPS data has highlighted the importance of geodetic measurements for estimating strain accumulation as well as seismic and aseismic moment release. Examples of complexity in elastic strain accumulation that cannot be inferred from earthquakes alone include partial and/or heterogeneous fault frictional locking [*Flück et al.*, 1997; *Mazzotti et al.*, 2000; *Sagiya*, 1999] and aseismic slip events or slow earthquakes [*Hirose et al.*, 1999; *Ozawa et al.*, 2001; *Dragert et al.*, 2001]. This study examines

continuous and survey GPS data from Guerrero, Mexico, where an earlier study of data from a single continuous GPS site showed evidence of transient deformation [*Lowry et al.*, 2001] and where seven continuous sites recorded a large aseismic slip event in 2002 [*Kostoglodov et al.*, 2003].

[3] GPS measurements in Guerrero consist entirely of episodic surveys prior to 1997, and only eight continuous GPS sites were operating in the region as of mid-2001 (Table 1). The possible presence of transient slip events in the early portion of the geodetic record greatly complicates interpretation and modeling of the survey data. Geodetic studies during interseismic periods typically assume that, in the absence of large earthquakes, displacements measured at infrequent intervals represent a steady state velocity. Transient aseismic slip typically occurs on timescales of a few weeks to a few years, and so can be aliased by infrequent survey measurements. In principle however, nonlinear slip dynamics should be recognizable in infrequently sampled measurements, so long as (1) the data are represented as a position time series rather than as a velocity vector, (2) spatial and temporal sampling are adequate to distinguish steady state from transient motions, and (3) transient motions are sufficiently large to distinguish from error in the GPS positions. GPS survey data sampled

¹Department of Aerospace Engineering Sciences, University of Colorado, Colorado, USA.

²Department of Physics, University of Colorado, Boulder, Colorado, USA.

³Instituto de Geofísica, National Autonomous University of Mexico, Mexico City, Mexico.

⁴Hutton Consulting, Seattle, Washington, USA.

⁵U.S. Geological Survey, Pasadena, California, USA.

Table 1. Guerrero GPS Stations Observed at More Than One Epoch^a

Station	Latitude, deg	Longitude, deg	Surveys							Continuous	
			92	95	96	98	00	01A	01B		
ACAP	16.79010	-99.87580	x	x	x	x	x	x	x	x	1999.91
AYUT	16.97748	-99.11601	x	x	x		x				
BAR1	17.59099	-101.42326				x	x				
C345	17.02000	-99.65544				x	x			x	
CAYA	17.04849	-100.26730				x	x	x	x		1997.02
CHIL	17.46382	-99.45846	x			x	x			x	
CPDR	16.77672	-99.62914				x	x				
CRUZ	16.72997	-99.12723	x		x		x				
DI16	16.90260	-99.76185				x	x				
EMU1	17.46796	-101.26016				x	x				
GC01	16.92700	-99.80678				x	x			x	
IGUA	18.39203	-99.50238					x	x	x		2000.43
LAGU	17.29646	-100.88290				x	x				
LAJA	17.13838	-100.39159	x		x	x	x	x			
LOMA	17.27858	-100.89177	x		x	x	x				
MONA	16.70865	-99.45708				x	x				
OAXA	17.07268	-96.73304						x	x		2001.16
PAPA	17.29951	-101.05165				x	x				
PENJ	17.01323	-100.11734	x		x	x	x	x			
PIED	16.75791	-99.64540	x		x						
PINO	16.39278	-98.12735						x	x	x	2000.52
POCH	17.36317	-100.82321	x		x		x				
POSW	19.00966	-98.65654			x	x	x	x	x	x	1996.32
SANM	16.77467	-99.43679	x	x	x	x	x				
TAXT	18.47588	-99.58040	x				x				
TCOL	17.18130	-99.54180	x			x	x			x	
TETI	17.16816	-100.62532	x		x	x	x				
TIGR	17.44908	-100.77000	x		x		x				
TLAC	17.69728	-99.94602	x				x				
TLAP	17.53745	-98.65230	x								
UNIO	16.80151	-99.12342	x	x	x		x				
YAIG	18.86243	-99.06694					x	x	x		1999.13
ZIHU	17.60585	-101.46398					x	x	x		2000.51

^aSurvey epochs were March 1992, September 1995, April 1996, November 1998, October 2000, October 2001, and November 2001. Dates for permanent stations represent the beginning of continuous operation.

at intervals of months to years have been successfully applied to studies of postseismic slip on faults when these criteria are met [e.g., *Segall et al.*, 2000; *Hutton et al.*, 2001; *Owen et al.*, 2002]. The combination of continuous and survey mode GPS data in Guerrero suggests that at least two aseismic transient slip events occurred prior to the large, well-documented event in 2002 [*Kostoglodov et al.*, 2003]. These include apparent postseismic slip following the 1995 $M_w = 7.3$ Copala earthquake as well as the 1998 event previously described by *Lowry et al.* [2001]. In this paper we examine steady state slip on the Guerrero megathrust and explore the distributions of transient slip that can fit the GPS measurements.

2. Seismotectonics of Guerrero

[4] The Middle America trench defines the boundary between the subducting Cocos and overriding North American plates. NUVEL1-A [*DeMets et al.*, 1994] convergence rates vary from 5.2 cm/yr at ZIHU to 5.9 cm/yr at CRUZ (Figure 1) and are directed N33°E. The slight (~12°) obliquity to the trench normal yields about 1.1 cm/yr of left-lateral motion across the plate boundary. The geometry of the subducting Cocos plate has been examined by many researchers [*Burbach et al.*, 1984; *Suárez et al.*, 1990; *Singh and Mortera*, 1991; *Pardo and Suárez*, 1995; *Kostoglodov et al.*, 1996]. Early work estimated a Wadati-Benioff zone from teleseismic hypocentral locations and inferred a

shallowly dipping (12–15°) planar subduction geometry beneath Guerrero state [*Burbach et al.*, 1984]. Later investigations include hypocenters derived from a permanent local seismic network and other geophysical data [*Suárez et al.*, 1990; *Pardo and Suárez*, 1995; *Kostoglodov et al.*, 1996]. These indicate that the subduction megathrust has an initial dip of <15° which steepens to as much as 30° near the coast and subsequently becomes subhorizontal beneath the overriding continental lithosphere (Figure 2).

[5] Bathymetry of the Cocos plate is nonuniform, with the Orozco and O’Gorman fracture zones trending nearly normal to the trench near the western and eastern boundaries of the GPS network, respectively. These physiographic features approximately define the boundaries of the Guerrero seismic gap, as it was originally identified by *Nishenko and Singh* [1987] prior to the 14 September 1995 $M_w = 7.3$ Copala earthquake. *Ortiz et al.* [2000] define a northwest segment (~260°E to 258.8°E), possibly corresponding to the rupture area of the 16 December 1911 ($M_s = 7.8$) event, and a southeast segment (261°E to 260°E) which correlates with the rupture areas of the 28 July 1957 ($M_s = 7.8$) and 15 April 1907 ($M_s = 7.9$) events (Figure 1). The northwest segment has not released significant seismic energy for more than 90 years, while post-1957 seismicity in the southeast segment includes a doublet of $M_w = 7.0$, 7.1 ruptures near Acapulco in 1962 and the $M_s = 6.9$ San Marcos event in 1989. The seismogenic zone in the latter region is shallow compared to worldwide averages [*Pacheco et al.*,

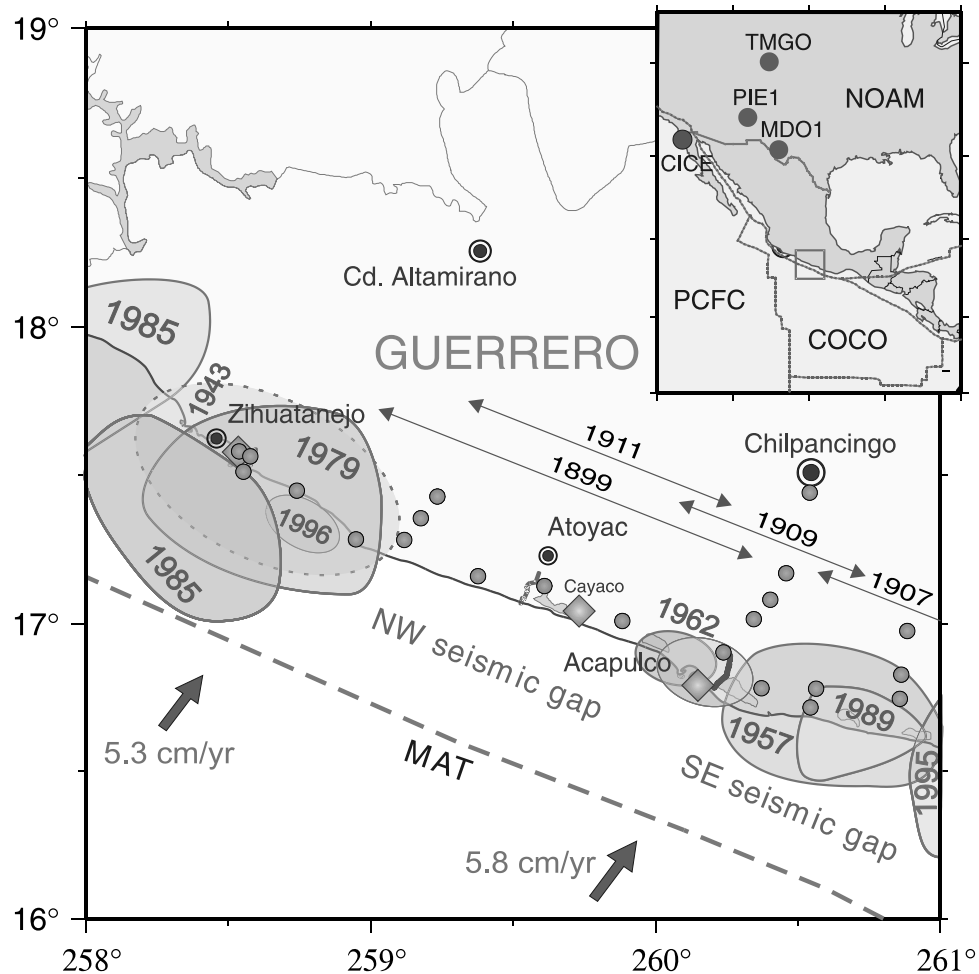


Figure 1. Inset: Tectonic setting of the Guerrero geodetic network. Plate boundaries and Pacific (PCFC), North America (NOAM), and Cocos (COCO) plate names are in bold. Arrows indicate the direction and magnitude of NUVEL1-A relative plate motion [DeMets *et al.*, 1994]. North American GPS sites used later in the analysis are also shown. The Guerrero region is shown by the square and in the expanded plot. Survey GPS sites are shown as circles and continuous GPS sites operating during the period of investigation are shown as diamonds. Major earthquake slip zones are shown with the year of the event. Inferred extent of rupture for earthquakes that predate seismic instrumentation are shown by the double-headed lines.

1993; Suárez and Sánchez, 1995], with hypocenters of large subduction thrust events generally less than 25 kilometers deep.

3. Geodetic Observations and Analysis

3.1. Survey GPS

[6] Initial GPS measurements of a 21 station network were made in 1992 (Table 1 and Figure 3). A primary reference site was established at ACAP, and this site has been occupied at nearly all epochs throughout the nine years of surveys in the region. The occupations for the 1992 survey lasted for 6 to 8 hours on 2 to 3 days at each site. The sites extend along the Guerrero coastline, with a few perpendicular profiles along Highway 95 connecting Acapulco to Mexico City, as well as along lesser roads connecting CRUZ to AYUT (at the eastern edge of the network) and LOMA to TIGR (at the western edge of the network). Elsewhere, inland regions of the Sierra Madre del

Sur are difficult if not impossible to reach by ground transportation. A few inland sites north of the mountain range (TLAP, TLAC, and TAXT) were observed, but reobservations of these sites are few because of the significant travel time and logistical effort required to include them.

[7] Four of the GPS sites established in 1992 were resurveyed following the 14 September 1995 Copala earthquake. ACAP and sites nearest to the epicenter (SANM, UNIO, AYUT) were occupied over a two day period, 12–13 days after the earthquake. Another partial resurvey was conducted in April 1996, including all of the sites occupied in 1995 and eight other sites along the Guerrero coast. A larger survey was conducted in November 1998. At this epoch, eight of the original sites were reoccupied, and ten new sites were installed and measured, extending the network northwest along the coast as far as ZIHU. All of the 1998 network sites and fifteen of the original 1992 sites were resurveyed in October 2000. Two much smaller

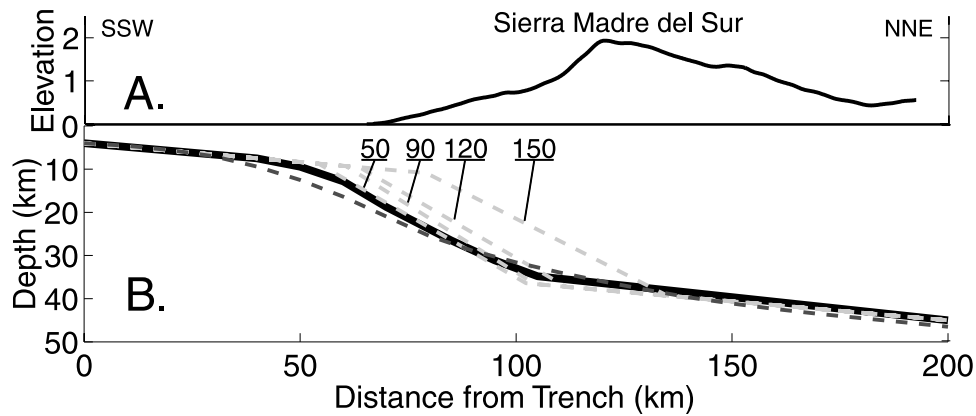


Figure 2. (a) Elevation profile, averaged along strike of the Guerrero segment of the plate boundary, vertically exaggerated 10×. (b) Estimates of geometry of the subduction slip interface in Guerrero. The dark shaded dashed line is from *Suárez et al.* [1990]; light shaded dashed lines are from *Kostoglodov et al.* [1996] with distance west from ACAP to the profile in km as indicated. Models described in this paper use the geometry given as a thick solid line.

surveys were conducted in October and November 2001 (Table 1).

3.2. Continuous GPS

[8] The first continuous GPS site in Guerrero was established at CAYA in January 1997. A second receiver (YAIG) was installed northeast of Guerrero, in the state of Morelos, in February 1999; continuous instrumentation was subse-

quently installed at ZIHU, ACAP, and IGUA in summer-fall 2000. Permanent stations were installed in the neighboring state of Oaxaca at PINO and OAXA in 2000 and 2001, respectively. Further details of the continuous GPS network in Guerrero is given by *Kostoglodov et al.* [2003]. GPS receivers have also been installed to study deformation at Popocatepetl volcano, about 275 km north from the Guerrero coastline. Two receivers (POSW and POPN) were

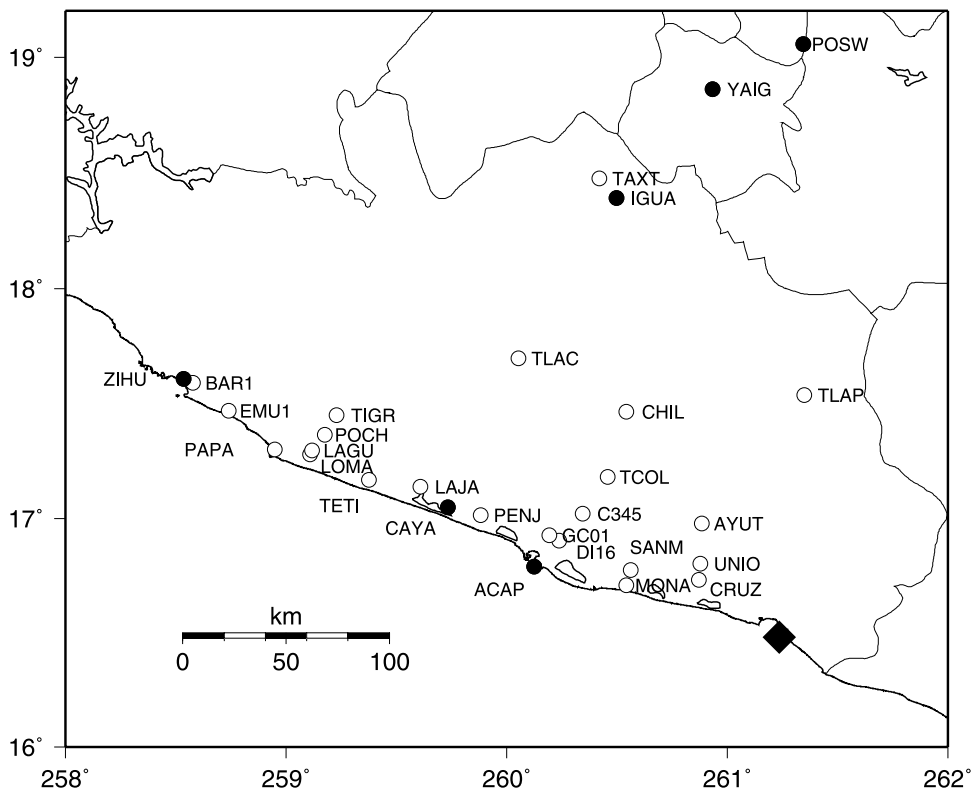


Figure 3. Repeated survey (open circles) and continuous GPS sites (solid circles) in the state of Guerrero and surrounding regions. Measurement histories are given in Table 1. The epicenter of the 1995 Copala earthquake is shown as a solid diamond.

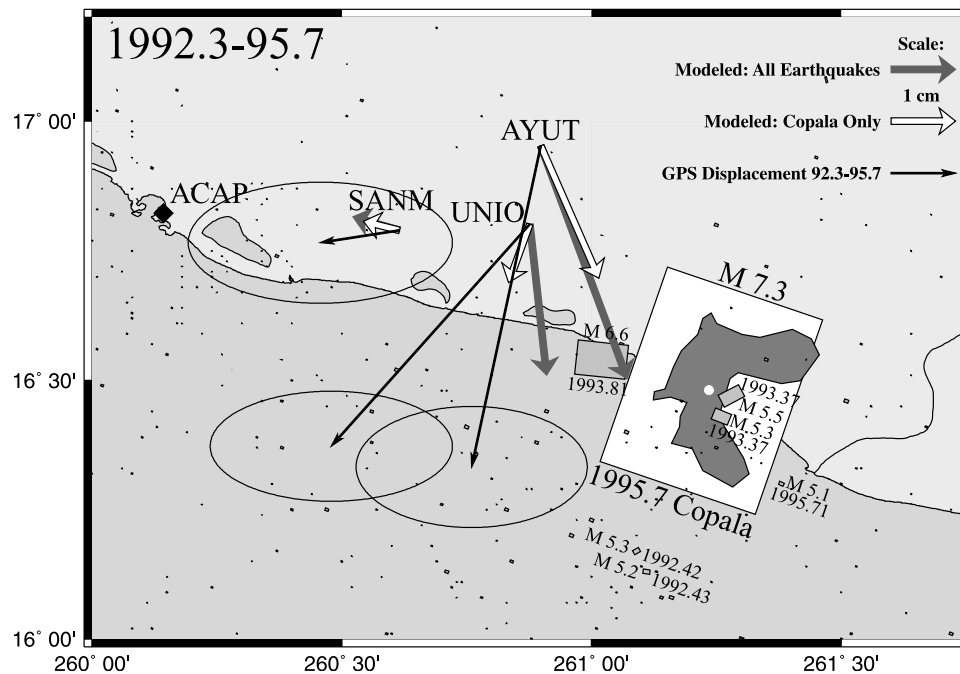


Figure 4. Seismicity and GPS displacements during the 1992–1995 observation epoch. The irregular patch is the *Courboux et al.* [1997] 1 m contour of slip during the Copala earthquake; the open dot corresponds to the location of rupture initiation, and the open rectangle approximates their solution plane. Other earthquakes are shown as dark shaded rectangles with area approximately corresponding to area of slip on the megathrust. Arrows depict surface displacements measured with GPS (thin solid arrows with 95% error ellipses), modeled for the Copala earthquake (thick open arrows), and modeled for all earthquakes (thick shaded arrows).

installed in mid-1996, and the former provides a relatively continuous record between 1996 and 2001.

3.3. GPS Data Analysis

[9] The GPS data were analyzed with the GIPSY-OASIS software package [Lichten and Border, 1987]. Orbits produced by the Jet Propulsion Laboratory were used to define the satellite coordinates in the ITRF2000 reference frame [Zumberge et al., 1997; Altamimi et al., 2002]. In the weighted least squares analysis of the GPS observations, receiver coordinates, clock values, and zenith tropospheric delays were estimated using standard estimation strategies [Larson et al., 1997]. Carrier phase ambiguities were resolved [Blewitt, 1989] at a high percentage of sites for all surveys except for 1992. All of the later surveys used receivers with dual frequency pseudorange, which aids ambiguity resolution. In the 1992 survey, receivers recorded C/A code pseudorange only, which is limited to one frequency. The 1992 survey is intrinsically weaker than the later surveys because GPS orbits were much less accurately determined at this time compared with later surveys. This is primarily due to the lack of global GPS tracking sites.

[10] Other continuous GPS sites were regularly included in the Guerrero network solutions to improve ambiguity resolution and to tie the Guerrero network to sites on the North American plate. These sites included McDonald Observatory, Texas (MDO1), Table Mountain, Colorado (TMGO), and Pie Town, New Mexico (PIE1) (Figure 1). As these sites were not installed until the mid-1990s, they could not be used in the 1992 solutions. Additional infor-

mation about the North American sites is available from the International GPS Service [Beutler et al., 1994].

4. Evidence for Transient Displacements

[11] During the March 1992 to November 2001 interval considered here, deformation of the Guerrero network was perturbed by the $M_w = 7.3$ Copala earthquake and six other $M_w \geq 6$ earthquakes, as well as numerous smaller events [Courboux et al., 1997; Cocco et al., 1997; Singh et al., 2000]. In addition, the GPS data show evidence of two aseismic slip events, including the 1998 event seen at CAYA [Lowry et al., 2001] and an earlier event during the 6-month period between measurements in late September of 1995 and April of 1996.

4.1. Coseismic Deformation at Survey Sites

[12] There have been several large earthquakes near the GPS network since the first epoch of survey measurement. The largest of these was the $M_w = 7.3$, 14 September 1995 Copala earthquake. A rectangular dislocation that best fit broadband seismograms and local strong ground motions [Courboux et al., 1997] is depicted as an open rectangle in Figure 4. A model of surface displacement relative to ACAP produced by the Copala moment release is shown by thick open arrows. Observed displacements for the 1992–1995 epochs including the earthquake (thin solid arrows in Figure 4) are substantially larger than predicted by the dislocation model. This is because the measurement period includes interseismic deformation and several other

earthquakes besides the Copala event, including a M_w 6.6 event in late 1993 that was nearer the network sites.

[13] Predicting the effects of earthquake displacements in the Guerrero GPS data is difficult because the uncertainties in earthquake locations, moment tensors and slip distributions can introduce errors in estimates of displacement that are nearly as large as the displacements themselves. For example, epicentral locations in the Harvard centroid moment tensor (CMT) catalog, derived from global broadband data [Dziewonski *et al.*, 2001], differ by 10 to 100 plus km from those of the Servicio Sismológico Nacional (SSN) catalog, which incorporates local and regional travel times into its locations. The moment tensor data from the CMT catalog were combined with the hypocenter and magnitude estimates from Singh *et al.* [2000] and from the SSN catalog to approximate the coseismic displacements in the GPS network. Rectangular dislocations were assumed to have an interplate thrust mechanism for those smaller ($M_w < 5$) events that lacked a moment tensor estimate, and we approximated dislocation dimensions and uniform slip using a scaling relation [Sato, 1979]. Summing the dislocation models for all of the earthquakes during the 1992–1995 period results in substantially larger surface displacements, predominantly because of the contribution of the 1993 M_w 6.6 event. The model still differs significantly from the observed displacements, but the uncertainties in the seismic source parameters plus the unmodeled steady state deformation can account for the difference.

[14] Coseismic displacements were modeled at each GPS site using seismic source parameters for each of the earthquakes. Only two, the $M_w = 6.6$ earthquake in 1993 and the $M_w = 7.3$ Copala earthquake in 1995, produced modeled displacements in excess of 1 cm during measured epochs. In modeling transient and steady state slip in section 5, the GPS data are inverted for an unknown uniform slip during the Copala earthquake, using a rectangular dislocation closely approximating the solution from Courboux *et al.* [1997]. Two different approaches for dealing with deformation induced by other earthquakes are considered. In one approach, all coseismic deformation are modeled using source parameters derived from the SSN and CMT catalogs, and this deformation is subtracted from the GPS time series before solving for other parameters of slip. In the second approach, coseismic deformation other than that of the Copala event is ignored, and slip parameters are modeled using the measured GPS position time series. The results from these two approaches are compared in section 7.3.

4.2. Evidence for Transient Aseismic Fault Slip

[15] In addition to coseismic deformation in the east network sites between 1992 and 1995, the GPS data show evidence of aseismic fault slip events between the 1995 and 1996 epochs of measurement, and again in 1998. Lowry *et al.* [2001] described and modeled transient aseismic deformation observed in 1998 at CAYA. That study used measurements from the beginning of 1997 to late 2000. This paper extends the CAYA time series to 7 October 2001, when the $M_w = 5.8$ Coyuca earthquake occurred southwest of the survey site at Penjamo, followed soon after by another large transient event [Kostoglodov *et al.*, 2003]. The east, north, and vertical components of the CAYA

baseline with respect to MDO1 (1553 km) are shown in Figure 5. The time series is shown as a baseline because ambiguity resolution requires differencing to another receiver, common mode errors are minimized in a difference, and the positions of CAYA are thus provided relative to a site on “stable” North America.

[16] Transients observed on a single GPS instrument must be considered with caution. Transient motions can result from instability of the monument or localized mass-wasting phenomena. As GPS equipment ages, electronics failures can also introduce time-dependent biases, particularly in the vertical component [Haines *et al.*, 2001]. Monument instability or soil creep are readily dismissed as candidate processes for the 1998 signal at CAYA [Lowry *et al.*, 2001]. One commonly used mechanism to identify systematic GPS positioning errors is to vary the elevation angle cutoff [Larson *et al.*, 2001]. CAYA solutions were computed with elevation angle cutoffs of 15, 20, and 25 degrees; the characteristics of the CAYA positions did not change.

[17] Although no other continuous geodetic instrumentation was operating in Guerrero, the sites on Popocatepetl volcano (POSW and POPN) are consistent with transient deformation occurring in 1998. The positions of POSW relative to MDO1 are remarkably stable except that they exhibit a southward displacement of about 1 cm at the same time that transient deformation was observed at CAYA (Figure 6). POSW and POPN were displaced an identical distance in the same direction. Given that POPN and POSW were located on the north and southwest flanks of the volcano, such behavior is inconsistent with a local volcanic deformation source.

[18] As CAYA, POSW and POPN were the only continuous GPS sites in the region before 1999, information about the spatial location of transient slip relies heavily on survey GPS measurements. For obvious reasons, it is much more difficult to determine timing of a transient from survey mode measurements. Nevertheless, if the transient deformation in Guerrero is real, it should be apparent in the time series of survey site positions referenced to North America as well as at continuous sites. Solutions referenced to a local Guerrero site are more ambiguous, because transient deformation at the reference site (e.g., ACAP) could contaminate the relative observations, thus obscuring the true magnitude and locations of anomalous displacement. Survey GPS results are traditionally displayed as velocities with respect to a reference site; these velocities will also be contaminated if there is transient motion at the reference site.

[19] Guerrero survey positions can be estimated with respect to MDO1, although these coordinates are generally less precise than at the continuous sites because many of the survey sessions lasted for 7–8 rather than 24 hours. In Figure 7 the north component of the MDO1 baseline is shown for all sites that were observed in at least three surveys between 1995 and 2001. Guerrero observations for 1992 are not shown because the continuous MDO1 site was not installed until 1993. There are a few North American sites that were observed in 1992, but they are at a distance of 4000 km from Guerrero. Given the GPS orbit accuracy in 1992, discussed earlier, baseline components at 4000 km distances are not sufficiently accurate to compare with the

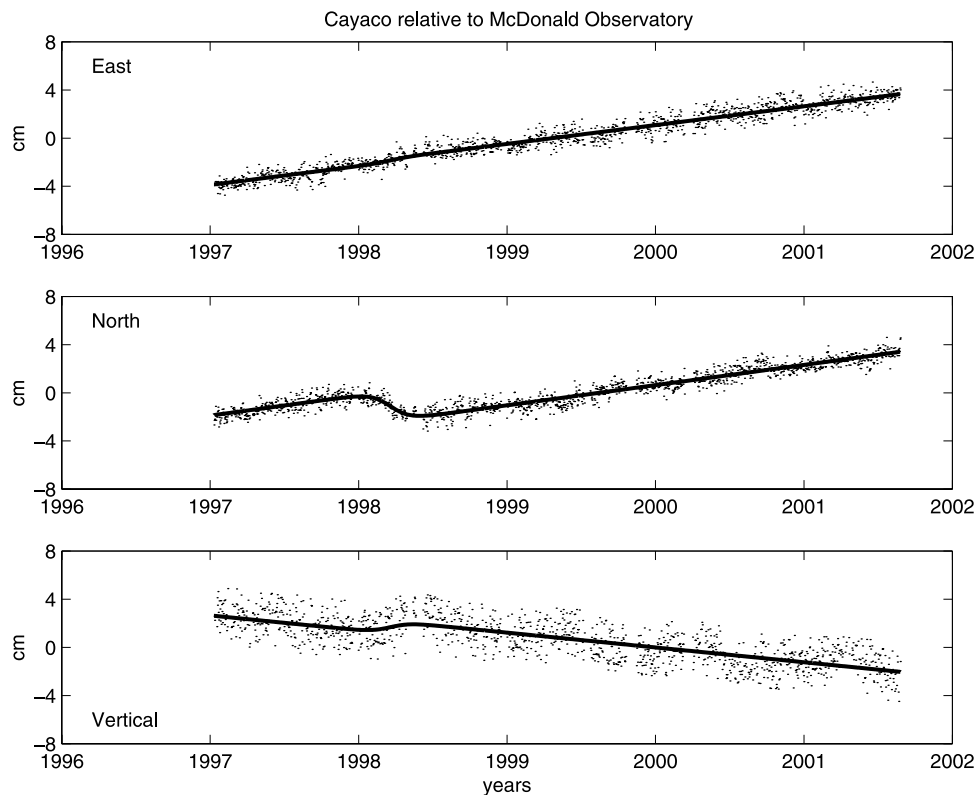


Figure 5. East, north, and vertical components of CAYA coordinates relative to MDO1. The solid curve is a best fitting hyperbolic tangent function superimposed on a line.

later more accurate baselines components available between 1995 and 2001.

[20] Sites at the bottom of Figure 7 are nearest the epicenter of the Copala earthquake, and sites higher in Figure 7 proceed northwest up the coast. Measurements from 1995 are significant outliers relative to steady state rates inferred from the other measurements, suggesting that transient slip occurred following the Copala earthquake. Transient deformation with magnitude similar to the CAYA anomaly occurred at PENJ, LAJA, LOMA, and TETI between 1996 and 1998, but the reversal of motion toward the south appears in the time series of survey measurements as a change in slope of the northward motion because the transient event is aliased by the temporal sampling.

[21] The total anomalous displacement during a transient event can be estimated from survey data if the temporal sampling is adequate to separate the transient motion from steady state velocity and from other transients. Such an estimate requires measurements before and after the transient, plus multiple epochs of measurement during a period of steady state motion. There is no evidence of transient deformation during the period from 1998 to 2000 when repeat measurements were made at a majority of the survey sites, so it is possible to solve for both steady state velocity and transient displacement at a few of the survey sites. For example, ACAP and SANM were observed often enough to estimate the displacements in both the 1995–1996 and 1998 transients, as well as the steady state velocity. Sites at LOMA, LAJA, PENJ, and TETI were sampled adequately to estimate displacement during the 1998 event; CAYA and POSW operated continuously throughout the 1998 event.

[22] To estimate anomalous displacements during transient events, a function is fit to the GPS coordinate time series of the following form:

$$\mathbf{x}(t) = \mathbf{x}_0 + \mathbf{V}t + \sum_{i=1}^n \frac{\mathbf{U}_i}{2} \left[\tanh\left(\frac{t - T_{0i}}{\tau_i}\right) - 1 \right] \quad (1)$$

in which $\mathbf{x}(t)$ are GPS site coordinates at time t , \mathbf{x}_0 are coordinates at a specified reference time, \mathbf{V} is steady state velocity, \mathbf{U}_i is anomalous displacement that occurred during the i th of n transient events, T_{0i} is the median time of the i th event, and τ is a temporal scaling that describes the period over which the event occurred. If T_0 and τ are specified, the other parameters can be estimated from linear least squares inversion. Using data at CAYA and POSW, a grid search was performed over T_0 and a gradient search was performed over τ to estimate optimal parameters for the 1998 transient of $T_0 = 1998.225$ and $\tau = 0.13$ years. We arbitrarily chose $T_0 = 1996.0$ and $\tau = 0.1$ for the earlier transient because, in the absence of continuous data, these parameters do not impact the displacement estimates so long as transient deformation begins and ends during the period between measurements.

[23] The linear parameters of steady state velocity and transient displacement were estimated via least squares minimization, weighted by the formal inverse variance of GPS coordinate estimates. Formal parameter uncertainties of velocity and displacement were then scaled to yield a reduced χ^2 parameter of one. The best fit hyperbolic tangent functions describing the CAYA time series are

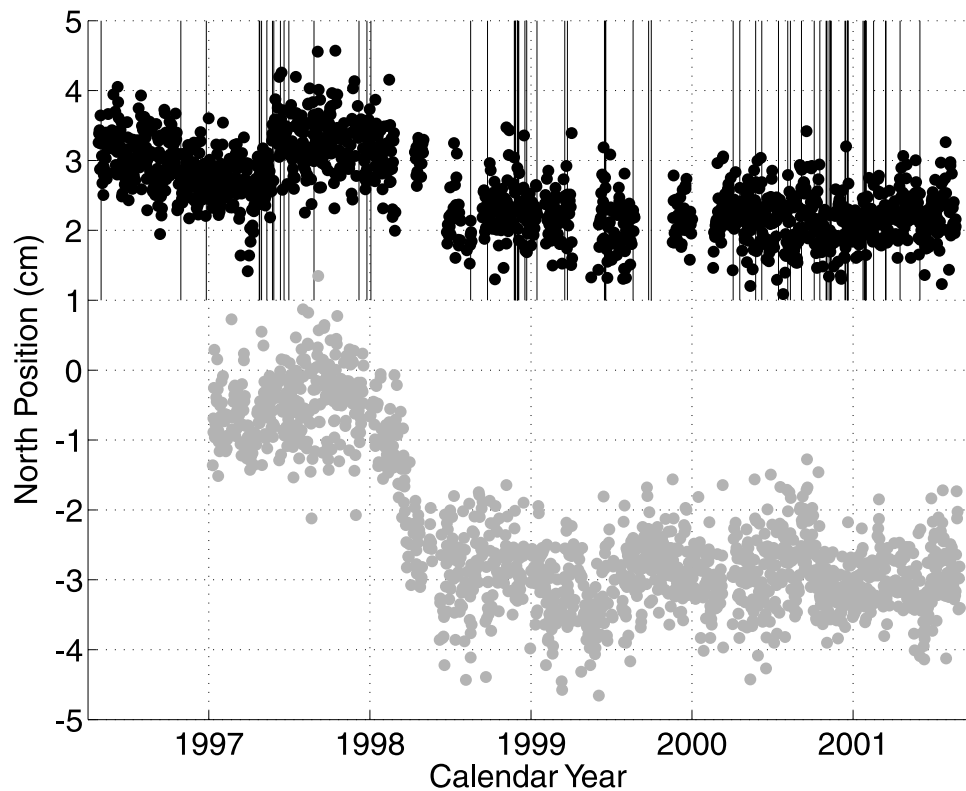


Figure 6. Daily north GPS coordinates at POSW (solid circles) and CAYA (shaded circles), relative to MDO1, after removing the respective steady state velocities. The vertical lines are minor to major explosions and eruptions compiled on the “volcano world” website (http://volcano.und.nodak.edu/vwdocs/current_volcs/popo/mar5popo.html). The 1 cm POSW displacement in 1997.35 correlates with reports of significant eruptive activity, but the ~ 1 cm motion between 1998.0 and 1998.5 occurred during a quiescent period.

shown in Figure 5. Horizontal displacements \mathbf{U} during the 1995–1996 transient are indicated as solid vectors in Figure 8. Displacements during the 1998 transient are shown in Figure 9. In both events the transient motions display magnitudes that are significant at 95% confidence and have directions consistently opposite the steady state velocity.

5. Slip Modeling of the Guerrero Data

[24] Clearly, both steady state and transient deformation contribute to the cycle of strain accumulation and seismic release in Guerrero. Consequently, an inverse model is described here that permits simultaneous solution for steady state slip on the plate interface and the location and timing of anomalous slip during transient events. This model has two main components: (1) a weighted least squares inversion for location, size, timing and slip in rectangular patches of anomalous slip on the plate-bounding megathrust, and (2) a constrained inversion for steady state virtual slip on the megathrust. The sum of these two models is compared to time series of GPS coordinates.

5.1. Data Used for Modeling

[25] Because this model involves a contribution from transient slip, we invert the time series of GPS position data rather than as velocities. In other words, all three

components of GPS position are modeled as a function of time. Coordinates used in this study are baseline coordinates, i.e., positions relative to another GPS site. Baselines relative to MDO1 are used for all of the continuous GPS sites, but survey sites are modeled using baselines referenced to MDO1 (for the 1995 survey and later) and referenced to ACAP (for all surveys) simultaneously. Baselines differenced to ACAP, the local reference site, yield more precise survey coordinates because a greater proportion of the error is common mode and thus cancels. However, baselines relative to MDO1 are included because otherwise the spatial aperture of the Guerrero network is too small to robustly constrain steady state and transient slip on the plate boundary. Baseline positions relative to ACAP are simulated by subtracting the model position at ACAP from the model position at the survey site. Baselines referenced to MDO1 are assumed to represent motion relative to the stable upper plate.

[26] Baseline GPS coordinates include a secular bias due to the difference in Cartesian velocity at the two sites resulting from rigid motion of a spherical tectonic plate. For Guerrero network sites referenced to MDO1, the bias introduced by rigid North American plate motion can be as large as 5.0 mm yr^{-1} in the east component, 2.2 mm yr^{-1} in the north and 1.1 mm yr^{-1} in the vertical. All baseline pairs were corrected for this effect by subtracting a velocity from the time series corresponding to the difference in NUVEL-1A

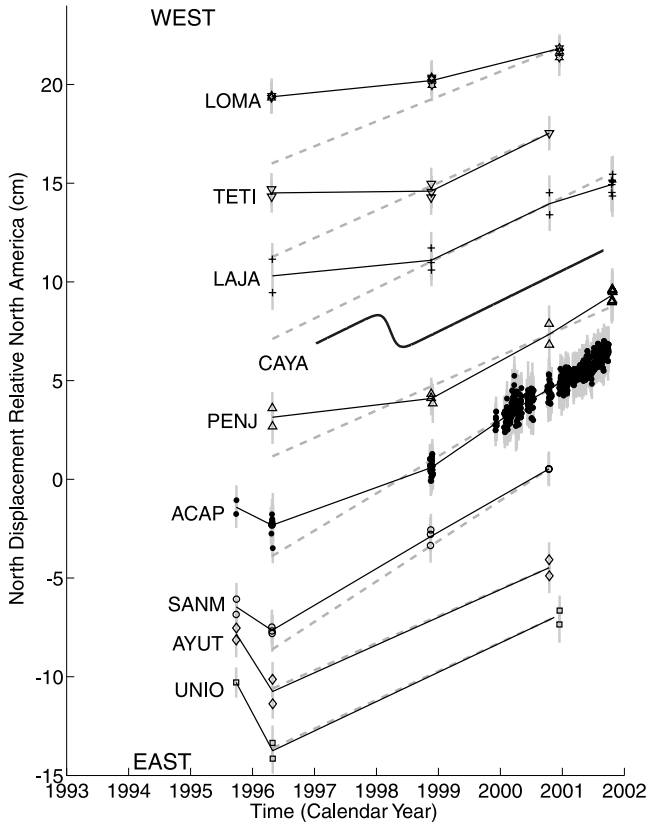


Figure 7. The north component of survey GPS sites relative to MDO1 with scaled 95% confidence error bars. The CAYA model fit is taken from Figure 5. Solid lines are linear fits to adjacent survey results. The dashed lines are from the best fit model of the steady state velocity described in section 5.

[DeMets *et al.*, 1994] NOAM site velocities transformed to east-north-up velocity at the differenced site.

5.2. Megathrust Geometry

[27] Earthquake hypocenters, moment tensors, and other geophysical data constrain the geometry of the megathrust in Guerrero [Suárez *et al.*, 1990; Kostoglodov *et al.*, 1996]. Interpretations differ slightly depending on the data used (Figure 2), but the observations require a very shallow dip ($\sim 7\text{--}12^\circ$) between the trench and the coastline, steepening to $20\text{--}30^\circ$ between the coast and about 50 km inland, and flattening (dip $\sim 5^\circ$) from there to the Mexican volcanic arc about 200 km further inland. The megathrust is approximated using a fault geometry intermediate between the various estimates, depicted as a thick solid line in Figure 2. There is evidence to support along-strike shallowing of the subduction interface between about 100–150 km west of ACAP [Kostoglodov *et al.*, 1996] (see also Figure 2), but the modeling performed here approximates the subduction megathrust geometry with no along-strike variations.

5.3. Transient Slip Deformation Model

[28] In the models of transient slip, GPS site coordinates $\mathbf{x}(t)$ are modeled using

$$\mathbf{x}(t) = \mathbf{x}_0 + \mathbf{V}t + \oint \mathbf{S}(\zeta, t)G(\mathbf{x}, \zeta)d\zeta. \quad (2)$$

Here, \mathbf{V} is constant velocity at the GPS site calculated from a steady state virtual slip model (described in section 5.4), ζ denotes location on the fault surface, G is the deformation Green's function [Okada, 1985], and \mathbf{S} is a functional describing the transient component of slip. \mathbf{S} is parameterized as a spatially uniform displacement on a patch of the megathrust that has a rectangular projection to the surface and time dependence described by

$$S(t) = \frac{S_0}{2} \left[\tanh\left(\frac{t - T_0}{\tau}\right) - 1 \right] \quad (3)$$

in which S_0 is the total transient slip. The slip model for a given transient event has just eight parameters, including timing parameters T_0 and τ , the along-strike length L and downdip width W of the slip patch, the center location (X_0, Y_0) of the patch, and the strike-slip and dip-slip components of total slip S_0^{ss} and S_0^{ds} , respectively.

[29] Transient slip parameters S_0^{ss} and S_0^{ds} can be linearly related to the GPS coordinate time series by calculating the GPS displacement response to a unit (1 meter) slip, scaling it through time using equation (3), and then solving via weighted least squares for the scaling factors S_0^{ss} and S_0^{ds} that minimize the difference between modeled and observed coordinates. The formal inverse variance of the GPS coordinate solution is used to weight each observation. Other parameters of transient slip do not relate linearly to the data, however, and so the weighted least squares solution for slip is combined with an adaptive grid search for optimal parameters of width, length, location and timing.

[30] The adaptive grid search approach is applied to cross sections of the model parameter space, using two nonlinear parameters at a time. Prior estimates of the 95% confidence limits on a given parameter are used to define the region of the parameter search. Confidence interval of a particular model parameterization is estimated from the minimum weighted root-mean-square (RMS) misfit R_{\min} between the best fit model and the data, using the likelihood ratio method of Beck and Arnold [1977]. Given zero mean, uncorrelated errors, the confidence region with probability α of containing the solution corresponds to the volume of the model parameter space for which

$$R^2 \leq R_{\min}^2 \left[1 + \frac{M}{n - M} \mathcal{F}_{\alpha}^{-1}(M, n - M) \right], \quad (4)$$

where M is the number of model parameters, n is the number of measurements, and \mathcal{F}^{-1} is the inverse of the F cumulative distribution function.

[31] The two-dimensional grid search for each pair of parameters is chosen to cover a region 1.5 times larger than the 95% confidence region estimated in previous runs, and is then discretized on a logarithmic scale such that the mesh at distal parameter nodes is 100 times larger than at the nearest nodes to the current estimate of best fit parameters. Parameters that are not being searched are fixed to the best fit model parameterization. The search begins at the initial estimate of best fit model and proceeds outward in a spiral pattern to more distal nodes. At each model node, a linear weighted least squares inversion is performed for six parameters of slip (S_0^{ss} and S_0^{ds} in each of three transient

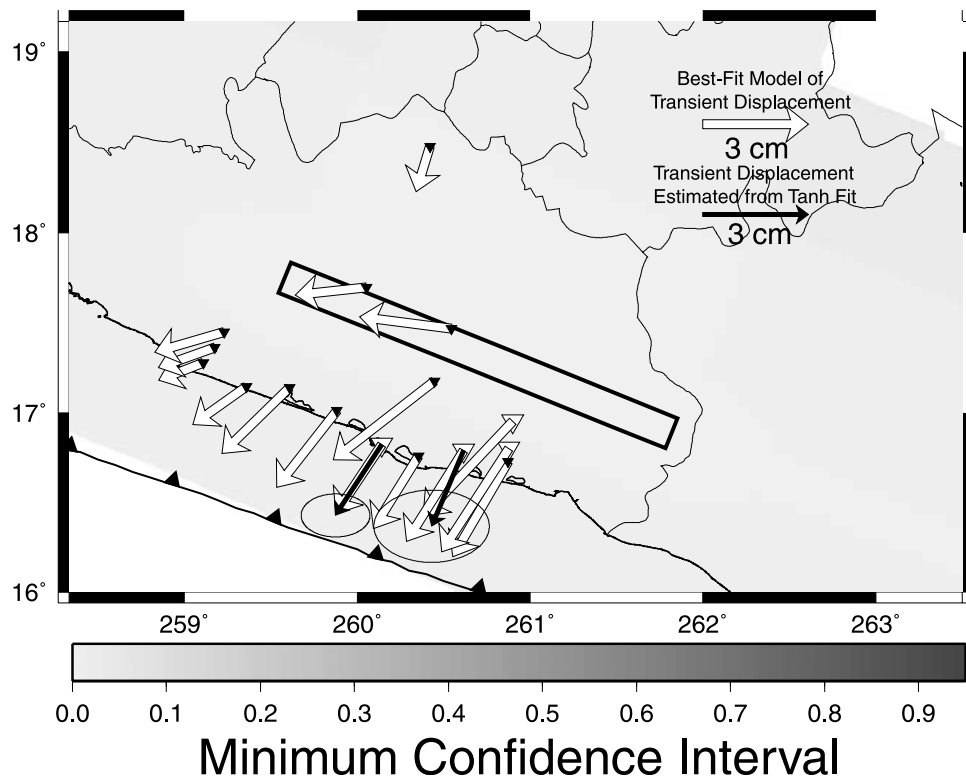


Figure 8. Model results for the 1995–1996 transient event. Solid vectors represent transient displacement from fitting equation (1) to the observed time series, with 95% confidence ellipse. Open vectors are from the best fit inversion of time series data for location and timing of transient slip. GPS sites sampled before and after the transient event are shown as triangles; the large open triangles indicate sites sampled in 1995 and 1996 (immediately before and after the event). Gray scale contours indicate the minimum confidence interval of all grid-searched slip models that activated a particular location on the thrust; the rectangle is the surface projection of the best fit model.

events). If the misfit R of the solution is smaller than the current estimate of R_{\min} , the two parameters of that model are retained as the new best fitting model of transient slip, and R_{\min} is set to R . Otherwise, if the model lies within the 95% confidence region, it is retained as a viable model. Models that are more than two nodes removed from the nearest viable model are skipped to save computational time, until the entire 95% confidence interval has been searched. The maximum and minimum model parameters within the 95% confidence interval of the search are saved to define future parameter search grids. All of the possible permutations of parameter pairs for a given transient are searched in turn, in an inversion sequence described further in section 5.5. The sequence searches throughout the entire nonlinear parameter space that fits the data at >95% confidence, so it is exceedingly unlikely that a local minimum will be mistaken for the global minimum.

[32] In this paper, we solve for parameters of three transient slip events: slip during the Copala earthquake, location/size and slip during the 1995–1996 transient event, and location/size, slip and timing of the 1998 event. Timing of the Copala earthquake is fixed to the seismically observed timing parameters, and the slip patch location/size is assigned to the open rectangle in Figure 4, after *Courboulès et al.* [1997]. There are no continuous sites to constrain

timing parameters of the 1995–1996 event, so $T_0 = 1996.0$ and $\tau = 0.1$ years are used to model that event.

5.4. Steady State Coupling Model

[33] The steady state component of GPS site velocities is modeled as constant-velocity slip on the subduction interface using a virtual slip approach, in which virtual slip or “back slip” with magnitude and direction equal and opposite the relative plate motion is used to represent frictional coupling on the megathrust [Savage, 1983]. Geodetic investigations commonly use this approach to apply the elastic half-space Green’s functions of *Okada* [1985] to model subduction megathrust coupling, in which plate boundary strain at greater depths is accommodated by viscoelastic flow [Savage et al., 1998; Sagiya, 1999; Darby and Beavan, 2001]. We discretize the megathrust at a 20×20 km scale within the area of densest Guerrero network coverage. Outside that area, a coarser discretization is used (Figure 10).

[34] On any given discrete segment of the megathrust, it is assumed that the steady state slip rate is some fraction of the relative plate motion. The direction and rate of Cocos–North America relative plate motion varies significantly within the study region, so relative plate motion is approximated as a constant within discrete segments and equal to the NUVEL-1A model prediction at the center of the segment. We solve separately for the coupling Φ^{ss} of the

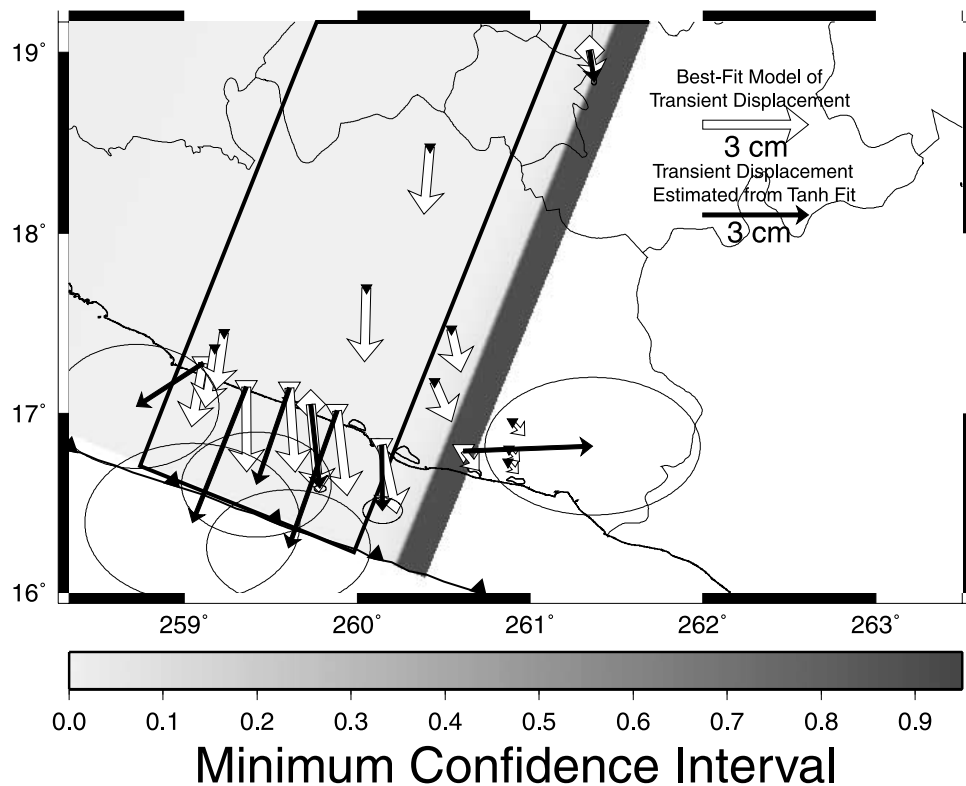


Figure 9. Model results for the 1998 transient event. Open diamonds represent continuous sites operating at the time of the event; other elements are the same as for Figure 8.

strike-slip component and Φ^{ds} of the dip-slip component, where $\Phi = S_b/S_{rpm}$, S_{rpm} is slip at the relative plate motion rate and S_b is the back slip rate.

[35] The 20 km discretization of the plate interface was chosen as the minimum scale on which we could reasonably expect to resolve slip variations, for reasons discussed further in section 7.1. This discretization of the plate boundary yields too many parameters to robustly constrain from site velocities using a standard least squares approach. Consequently, the solution space is restricted by imposing additional constraints. For example, the truly steady state slip on interseismic timescales requires $0 \leq \Phi \leq 1$. From the observation that oblique convergence commonly partitions as dip slip on shallowly dipping thrusts and transcurrent slip on steeply dipping strike-slip faults, we can also reasonably expect that $\Phi^{ss} \geq \Phi^{ds}$. Solutions of linear equations involving these kinds of constraint relations are most easily solved using a linear programming approach [e.g., Menke, 1984], so the coupling parameters are estimated using a simplex algorithm [Press et al., 1992]. The site velocity response is calculated for perfectly coupled back slip ($\Phi = 1$) on each segment. We then solve for the model that minimizes differences between the modeled and observed steady state components of GPS velocity in a weighted L_1 sense, subject to the constraints $0 \leq \Phi \leq 1$ and $\Phi^{ss} \geq \Phi^{ds}$. Because the linear programming approach requires an L_1 rather than L_2 minimization, the observations are weighted by the inverse standard deviation of the velocity measurement.

[36] In addition to the constraint equations described above, we also introduce a smoothing criterion C and require that neighboring coupling parameters $\Phi_a - \Phi_b \leq C$.

The purpose of the smoothing criterion is to reduce spurious spatial variance of coupling introduced by errors in the velocity estimates. We examined the weighted mean misfit of the steady state model to the residual velocities for smoothing criteria ranging from $C = 1$ (i.e., no smoothing) to $C = 0.2$ (i.e., resolution equivalent to a 100×100 km grid discretization). Misfit increases slowly and approximately linearly for $C = 1$ to $C = 0.5$ (from 1.15 mm yr^{-1} to 1.18 mm yr^{-1}), then much more rapidly to $C = 0.2$ (1.31 mm yr^{-1}). We use $C = 0.5$ for the smoothing criterion in results presented here, yielding resolution equivalent to a 40×40 km grid discretization.

5.5. Inversion Sequence

[37] GPS time series are modeled using a combination of linear weighted least squares inversion for transient slip, grid search minimization of a weighted root-mean-square error norm to optimize nonlinear terms in the transient model, and linear programming solution for steady state coupling coefficients Φ that best fit the residual velocities in an L_1 norm sense. The inversion sequence proceeds by the following steps.

[38] 1. A starting model is chosen to describe steady state coupling Φ on the megathrust and the nonlinear parameters of transient slip events, including size and location of the rectangular slip patch for the 1995–1996 and 1998 events, and timing parameters T_0 and τ of the 1998 event. For results shown in this paper the starting model of steady state coupling assumes completely coupled ($\Phi = 1$) segments within 75 km of the trench in Figure 10 and free slip ($\Phi = 0$) on segments further downdip. Starting models of transient

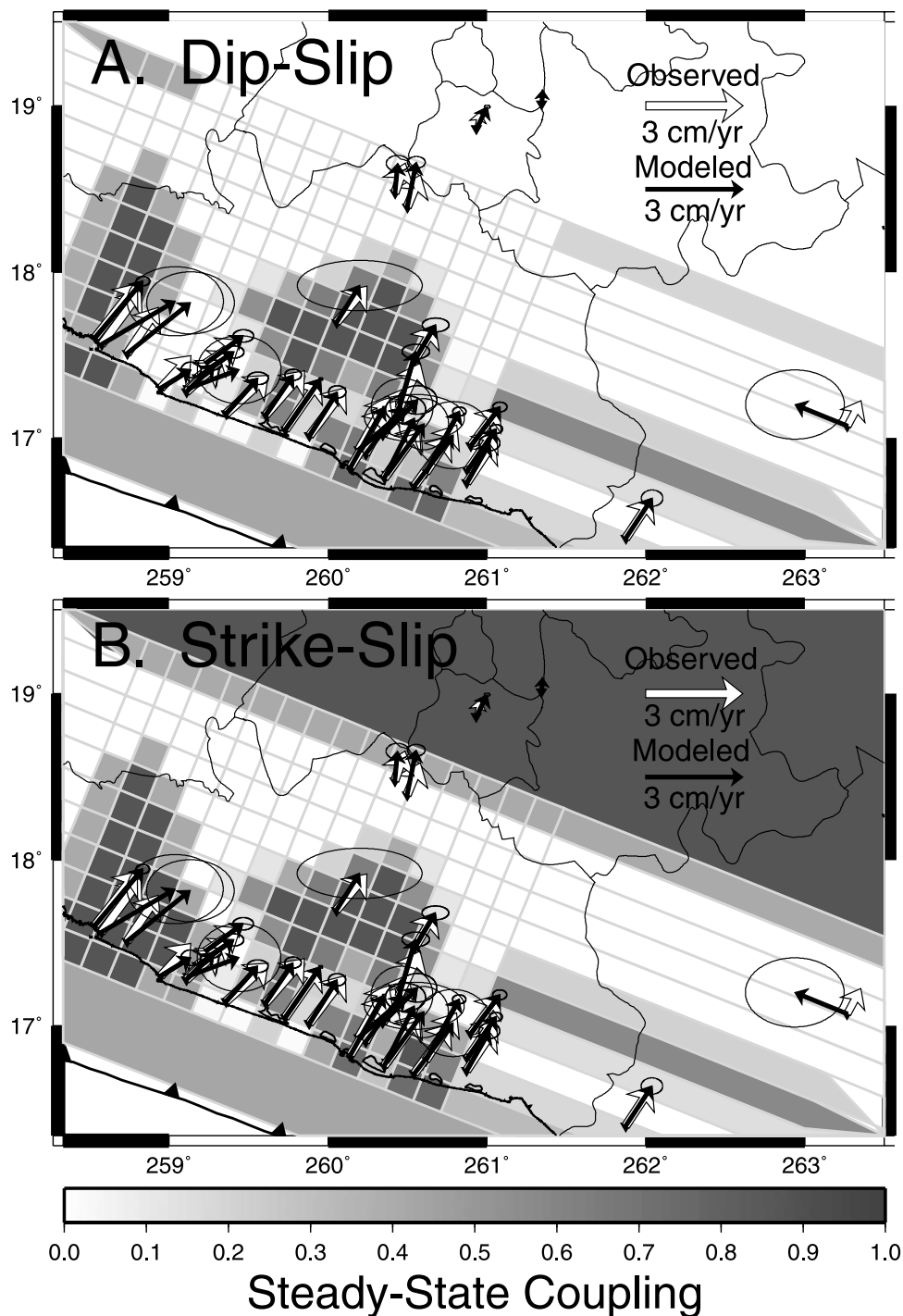


Figure 10. Best fit model of steady state coupling. Open vectors represent the best fit steady state velocity model; solid vectors (with 95% error ellipses) are calculated from residuals of the transient slip modeling. Gray scale shading represents (a) fraction of dip-slip coupling; (b) fraction of strike-slip coupling.

slip use a rectangular slip patch with length $L = 200$ km and width $W = 50$ km, centered at ACAP, for both the 1995–1996 and 1998 events. The 1998 event also had initial timing parameters $T_0 = 1998.225$ and $\tau = 0.13$ years, based on earlier modeling of the coordinate time series using equation (1). Other starting models were tried, but these were found to yield negligibly different final estimates of best fitting model parameters.

[39] 2. Parameters of transient slip are estimated using the combination of weighted least squares inversion and adaptive grid search described in section 5.3. A steady state velocity is calculated and subtracted for the current best fit model of megathrust coupling from each of the GPS time series. A grid search is then performed over each of the possible permutations of paired model parameters (X_0 , Y_0 , L , W) of the 1995–1996 transient, a total of six grid

searches, retaining the model parameters that minimize the weighted RMS misfit. Next a grid search is performed over each permutation of paired parameters (T_0 , τ , X_0 , Y_0 , L , W) of the 1998 transient, totaling fifteen grid searches. When the grid searches are complete, new estimates of steady state velocity are calculated from the residuals of the GPS time series minus the best fit model of transient slip to use in a new solution for steady state coupling on the megathrust.

[40] 3. Megathrust coupling is estimated using the linear programming approach described in section 5.4. The best fit model estimates of steady state velocity are retained to use in the model of transient slip (step 2).

[41] 4. The solution is iterated, continuing from step 2, until the error norms for the transient slip and steady state coupling models achieve a stable minimum. Starting models examined for this paper required between 8 and 20 iterations to converge.

6. Model Results

[42] Time series comparing the best model fits with daily GPS measurements are depicted in Figures 11 and 12 for a few representative baselines relative to MDO1 and ACAP, respectively.

[43] Spatial locations of the best fit models of transient slip are shown as rectangles in Figures 8 and 9 for the 1995–1996 and 1998 events, respectively. Both of the best fit models have slip centered down-dip of the seismogenic portion of the megathrust (compare for example with Figure 1). However, these are not the only models that are permitted by the available data. Figures 8 and 9 also depict, as shaded regions, all of the other regions of the plate interface where the grid search produced a slip model that was able to fit the data within the 95% confidence interval.

[44] The best fit model predictions of transient displacement compare favorably with the measurements from fitting equation (1) to the survey data at ACAP and SANM in the case of the 1995–1996 event. In the 1998 event, the best fit displacements at POSW, CAYA and ACAP closely match the independent estimates from fitting equation (1) to the continuous data, but the fits to independent estimates from survey data at LAJA, LOMA, TETI, PENJ and SANM are poorer. This is because the continuous site data dominate the solution for transient slip, owing to the much smaller uncertainties inherent in larger numbers of observations. Observed displacement vectors are shown in Figures 8 and 9 only for those sites with sufficient temporal sampling to confidently separate steady state velocity from each of the transient displacements using equation (1). Hence AYUT and UNIO, which exhibit significant southward and upward motion during the 1995.7 to 1996.3 epochs (Figures 7 and 12d), are not depicted with observed displacement vectors in Figure 8 because there was no 1998 epoch of observation to separate the steady state velocity from 1995–1996 and 1998 transients. However, the sites with observed displacement vectors are not the only sites that contribute to the solution. All of the sites designated with an open model vector were measured before and after the transient of interest, and thus (for reasons discussed further in section 7.1) all of those sites contribute to the solution for the transient event.

[45] Best fit results of the solution for steady state velocity are shown in Figure 10. Almost all of the velocities measured from residuals of the transient models agree with the best fit model at 95% confidence. The model suggests that the seismogenic megathrust is about half frictionally coupled ($\Phi = 0.52$), and portions of the megathrust further downdip exhibit partial to complete coupling as well. Dip-slip frictional coupling is negligible beyond about 200 km from the trench, and strike-slip coupling is similar to dip-slip over most of the plate interface.

7. Discussion

[46] Many of the survey sites used in this study were measured at only two, three or four epochs (Table 1). If two transient deformation events occurred during the 1992.23–2001.75 period of analysis, modeling the displacement time series at a particular site via equation (1) requires a minimum of four parameters to describe the steady state slope, intercept and two transient displacements. If we were to try to model equation (1) independently at each individual site, only two sites in the network (ACAP and SANM) have sufficient temporal sampling to estimate both the 1995–1996 and 1998 transient displacements plus a steady state velocity. Guerrero state is just one of many subduction zone localities where tens to hundreds of thousands of dollars were spent to collect survey GPS measurements before subsequent continuous GPS measurements indicated transient slip behavior. Ideally, we would like to make use of these data rather than to simply discard them. Hence a major objective of this paper is to assess the feasibility of using survey data to extend the record of slip behavior prior to continuous GPS measurements.

7.1. Motivation and Implications of the Steady State Coupling Model

[47] Our primary motivation for modeling steady state plate coupling is to use the network spatial redundancy to partially compensate for sparse temporal sampling in the early Guerrero survey data. The coupling model can be considered as a means by which to smoothly interpolate steady state velocity estimates from well-sampled sites to poorly sampled sites, thus enabling a more robust estimation of transient displacements at those sites. The velocity field generated by any physically reasonable steady state coupling on the plate interface must vary smoothly because the surface deformation response to a point dislocation has a spatial wavelength roughly twice the depth of the dislocation, and the Guerrero plate interface is relatively deep where we have GPS sites (ranging from 20 km depth below coastal sites to ≥ 80 km below inland sites such as IGUA and YAIG, e.g., Figure 2). Consequently, closely spaced GPS sites should have very similar steady state velocities.

[48] Consider for example the site TAXT, observed during the 1992.2 and 2000.8 epochs. If we had chosen to model the GPS displacement time series using equation (1), and then use those velocities and displacements to model slip, we would simply discard the data because temporal sampling is insufficient to distinguish the steady state velocity or the transient displacements. However, the steady state velocity at continuous site IGUA is well-determined, and as the two sites are separated by only about ten km over

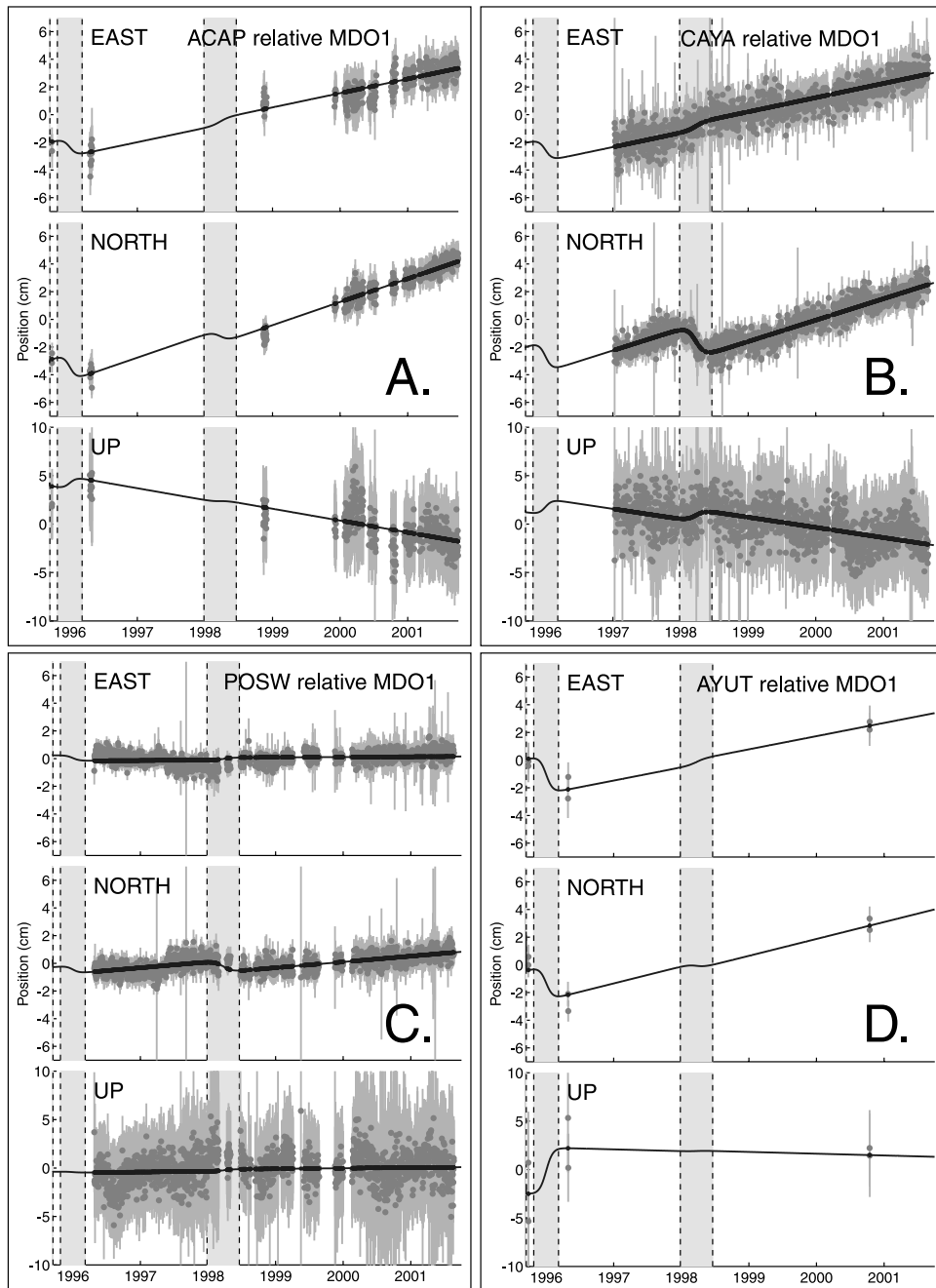


Figure 11. Best fit model time series of baseline coordinates relative to MDO1 for (a) ACAP, (b) CAYA, (c) POSW, and (d) AYUT. Shaded circles are GPS coordinates, shown with scaled 95% uncertainties (light shaded bars). Solid line is the best fit model time series for displacement at each site. The very light shaded areas bounded by dashed lines indicate periods of transient displacement.

a plate interface at ~ 80 km depth, their velocities cannot differ by more than ~ 1 mm/yr. Hence, in the global model used here, we have an additional constraint that the total displacement between measurement epochs at TAXT must equal the sum of the two transient displacements plus steady state displacement at approximately the rate observed at IGUA. Without such bootstrapping of constraints in the context of a global model, most of the survey data prior to 1998 would have to be discarded, and there would be no constraint of the transient events at any of the sites denoted by solid inverted rectangles in Figures 8 and 9. The

remaining sites (i.e., those with solid “observed” displacement vectors) are too few and too sparsely distributed to invert.

[49] Because the main objective of the coupling model is to better constrain the transient displacements at poorly sampled survey sites, we consider the coupling parameters shown in Figure 10 to be of secondary importance in results reported here. Large localized variations in coupling will produce small gradients in surface velocity field, so the spatial resolution of steady state plate coupling is rather poor and estimates of individual coupling parameters are

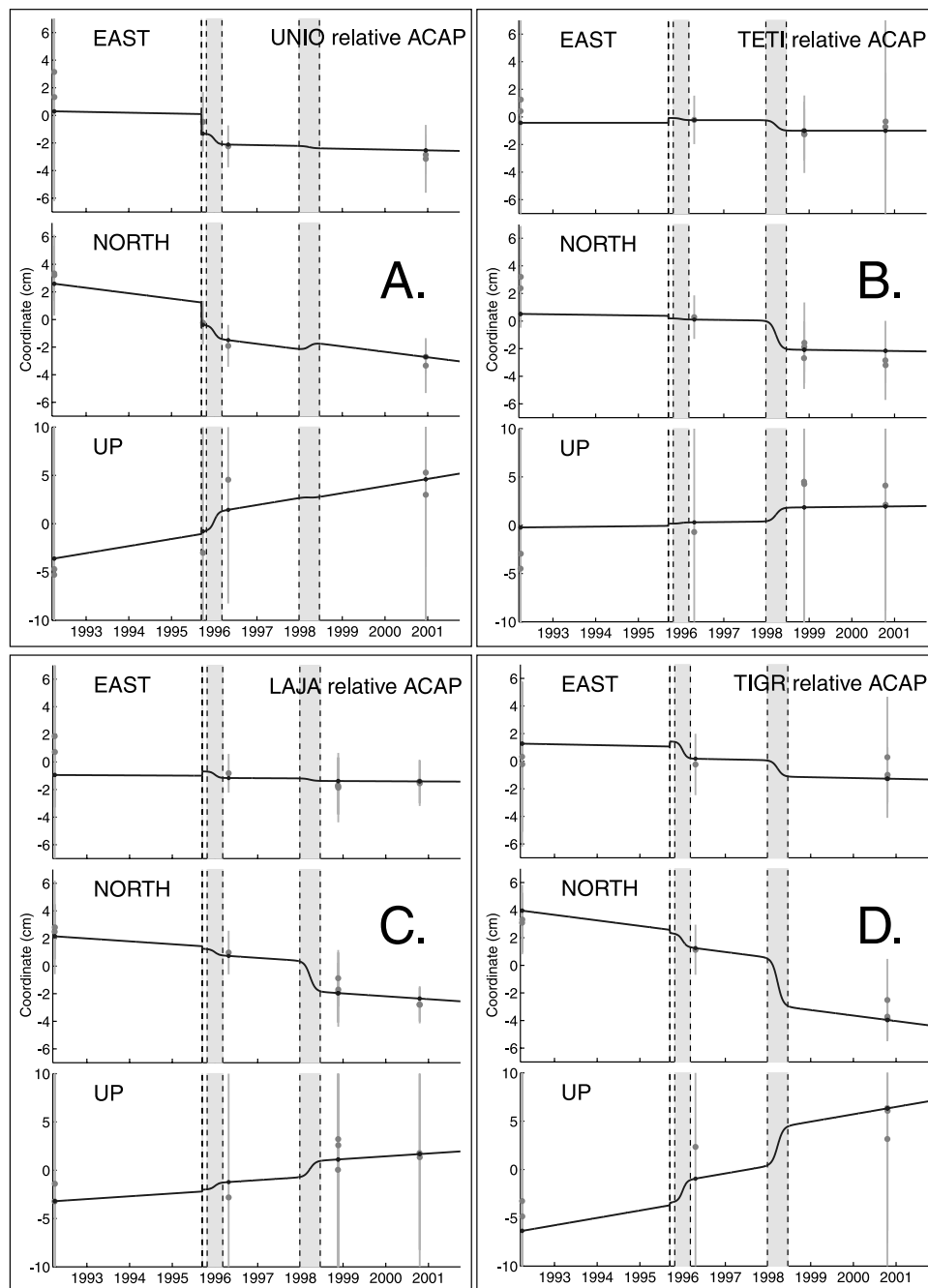


Figure 12. Best fit model time series of baseline coordinates relative ACAP for sites (a) UNIO, (b) TETI, (c) LAJA, and (d) TIGR. See Figure 11 for description.

sensitive to measurement error in the GPS velocities. However, averages of coupling estimates over large, well-sampled regions will be approximately correct (hence the decision to impose a smoothing criterion in the inversion), and the physical constraints that coupling $0 \leq \Phi \leq 1$ and $\Phi^{ss} \geq \Phi^{ds}$ also substantially limit the possible solution space. Consequently, errors in the estimate of remainder transient displacements due to errors in interpolation of the steady state velocity field should be small.

[50] Exploitation of the steady state constraint relations requires a linear programming solution, but that approach does not lend itself to straightforward estimation of param-

eter error. In future analyses, we will assess the parameter error via Monte Carlo simulation of the effects of Gaussian error in the velocity estimates. In this paper, we show the steady state coupling parameters in Figure 10 with the caveat that some small-scale variations (particularly on deeper segments) may reflect error in the residual estimates of steady state velocity rather than true variations in plate coupling. Nevertheless the larger-scale variations in well-sampled regions undoubtedly reflect real coupling behavior. We can infer with some confidence that the shallow seismogenic portion of the plate-bounding thrust is partially coupled (with integral coupling coefficient $\Phi \sim 0.5$) and the

down-dip region where the slab flattens and transient slip appears to focus is also strongly coupled (a necessary condition to accumulate strain energy leading up to a transient slip event).

7.2. Significance of the Transient Events

[51] The best fitting centroid location, length, width and timing parameters of transient fault slip are determined from a grid search over several millions of possible models. In the course of the grid search, hundreds to millions of those models will intersect a given location on the fault surface, depending on the location. To characterize the parameter uncertainties of the models in a relatively simple visual fashion, we discretized the plate interface at a 1 km spacing and kept account of the minimum weighted RMS misfit R^2 of all the models that produced slip at each particular location on the plate interface. The gray scale shading in Figures 8 and 9 represents the minimum confidence interval among all of the grid-searched models that produced slip at the corresponding location, calculated from R^2 via equation (4). Locations that are unshaded (i.e., eastern regions in Figure 9) did not produce slip in any model that fit the data within the 95% confidence interval.

[52] The shading indicates that the boundaries of anomalous slip during the 1995–1996 event cannot be determined from the GPS observations at 95% confidence. The lack of constraint on the boundaries of slip during the 1995–1996 event does not necessarily mean that the data cannot rule out any model at high confidence, but we have also examined contour plots of model confidence as a function of model parameter and we find that no combination of (X_0, Y_0, L, W) examined in the grid search was rejected at >60% confidence. Models which fit the data also included normal faulting events. We expect that the most robust feature of this type of inversion should be the integral property describing moment release, given by $M_0 = \mu LW|S_0|$, where $\mu = 2 \times 10^{10}$ is shear rigidity and $|S_0|$ is the modulus of anomalous slip. The equivalent magnitude M_w for grid-searched models of the 1995–1996 event ranges from 6.1 to 8.4, and some of the smaller magnitude models produce negligible surface displacements at most of the network sites. Hence, while the best fitting model of $M_w = 7.1$ thrust slip down-dip of the seismogenic zone (Figure 8) is plausible, transient slip during 1995–1996 is not required at high confidence by the data. Reasons for the poor resolution of the 1995–1996 behavior include sparse temporal sampling prior to 1996, large uncertainties in early positions due to short observation windows and poor ambiguity resolution of the 1992 data, inconsistent spatial sampling (e.g., only four sites were occupied for short sessions in 1995), and parameter tradeoffs between the 1995 Copala earthquake and the subsequent slip.

[53] The 1998 event is better constrained by the available data. For example, no model that produces slip east of San Marcos can fit the data at >95% confidence, and if one looks at contour plots of confidence for the grid search of along-strike position X_0 versus length L , the eastern boundary of slip must be within ± 25 km of Acapulco. Other aspects of the spatial distribution of slip are poorly determined, except that the down-dip width must be at least 250 km. However, all of the grid-searched models have predominantly thrust slip, and the range of moment release

is much tighter than for the 1995–1996 event, with magnitude equivalent to a $7.0 \leq M_w \leq 7.5$ earthquake. Hence, although the spatial limits of slip are not entirely known, transient slip is required at >95% confidence to explain the 1998 behavior. It is not surprising that the 1998 event is better constrained than the 1995–1996 event, given the continuous measurements at CAYA and POSW.

[54] Proprietary continuous GPS data collected beginning in 1993 by the Instituto Nacional de Estadística, Geografía, e Informática (INEGI) provide further evidence that large transient slip events affected a large region of southern Mexico in 1995–1996 and 1998. In Figures 4 and 5 of *Marquez-Azua and DeMets* [2003], sites INEG, OAXA, and TOLU show evidence of 1–2 cm of southward displacement relative to the longer-term trend, coincident with the timing of the events described here from Guerrero network data.

7.3. Effects of Earthquake Displacements

[55] As noted in section 4.1, the GPS data are inverted using two approaches. In one approach, seismic displacements other than the 1995 Copala earthquake are modeled from catalog hypocenters and moment tensors and removed from the GPS data prior to modeling the remainder deformation. In the second approach, earthquake deformation was neglected. All of the figures and discussion reported to this point are taken from results for the second approach in which earthquakes other than Copala were ignored. The two approaches give very similar results, but the weighted RMS misfit with earthquakes neglected is smaller (4.82 mm versus 4.97 mm). This suggests that errors introduced by uncertainties in the seismic estimates of earthquake locations and moments are as large as or larger than the modeled displacements. The misfit when earthquakes are explicitly modeled exceeds the two-sigma confidence interval of the solution when earthquakes are neglected. However the most significant difference between the best fit models for the two cases is in the inverted slip S_0 during the Copala earthquake. The solution with earthquakes neglected yields a slip of 1.51 m for the Copala event, with a rake of 80.6° . With earthquakes included, the slip in the best fit model drops to 1.15 m with a rake of 71.5° . The reduction in slip occurs primarily because of subtraction of displacement during the 1993 $M_w = 6.6$ event (Figure 4). Slip inverted from strong ground motion data using a similar dislocation to that inverted here yielded average slip of 1.4 m and rake of 75° [*Courboux et al.*, 1997].

7.4. Broader Implications

[56] The Guerrero segment of the Cocos-North America plate boundary has long been recognized as a seismic gap [*Nishenko and Singh*, 1987; *Suárez et al.*, 1990; *Kostoglodov et al.*, 1996; *Ortiz et al.*, 2000]. More than five meters of relative plate motion has occurred since the most recent large events in 1899 and 1911, and there remains some uncertainty as to whether even these were megathrust events [e.g., *Anderson et al.*, 1989]. Geodetic studies of the western Shumagin segment of the Alaskan plate boundary, for example, suggest that a seismic deficit may not necessarily translate to high seismic potential if slip is accommodated aseismically [*Lisowski et al.*, 1988; *Frey Mueller and Beavan*, 1999]. This study suggests $\sim 50\%$ frictional cou-

pling of the Guerrero megathrust above 30 km depth, which may represent either slip throughout the region at 50% of the relative plate motion rate, or slip at the relative plate motion rate on 50% of the area. The data presented here cannot rule out the possibility that slip during the transient events relieved some of the strain accumulation at depths <30 km, but models which activate slip at much greater depths are generally favored, and in the case of the 1998 event the centroid of slip is required to be downdip of the region generally activated in shallow thrust events (Figure 1). Hence earlier studies suggesting the potential for a large ($M_w \sim 8$) magnitude earthquake [Anderson *et al.*, 1989; Suárez *et al.*, 1990; Valdés-González and Novelo-Casanova, 1998] cannot be discounted.

[57] The best fit location of the 1998 transient slip event from modeling all of the available data is somewhat different from that reported by Lowry *et al.* [2001]. The differences in these models are not surprising given that the earlier model used only the CAYA data, and that the model parameterization of Lowry *et al.* [2001] assumed a slip patch which traveled along strike during the event. Data from a single continuous GPS site contain limited information about the spatial distribution of slip, and will be most sensitive to nearby slip. The modeling approach detailed here also has its limitations, as it assumes uniform slip and uniform time dependence everywhere on the rectangular patch, whereas the true slip is undoubtedly more variable in both time and space.

[58] Important questions remain as to the relationship of transient events in Guerrero to seismicity during these periods. The timing of the 1995–1996 event, although poorly constrained by the survey sampling, is consistent with initiation as postseismic slip following the Copala earthquake. Transient fault slip with large moment release is commonly observed following large earthquakes [e.g., Segall *et al.*, 2000; Hutton *et al.*, 2001; Owen *et al.*, 2002]. Aseismic slip in regions of transitional frictional properties is predicted by models of rate- and state-dependent friction in response to coseismic changes in static stress [e.g., Lapusta *et al.*, 2000]. However, the best fit model suggests that the 1995–1996 slip propagated from Copala to at least the westernmost sites measured in 1992 and 1996, a distance of ~ 200 km. Propagation of postseismic slip more than 100 km along strike was also observed following the 1997 $M_w = 7.8$ Kronotskoë earthquake [Bürgmann *et al.*, 2001]. The largest seismic event in southern Mexico near the initiation time of the 1998 transient was a $M_w = 5.9$ event just south of the Middle America trench at the longitude of the Copala seismic event. However, the static stress change west of Acapulco where the transient occurred would be small, making it a questionable candidate for a triggering event.

8. Conclusions

[59] We have presented a model of steady state and transient slip on the Guerrero megathrust, derived from both survey and continuous data sets. Transient displacements are modeled using combined linear and grid search inversion for uniform slip on a rectangular patch of the subduction megathrust, using weighted least squares. Steady state slip on the megathrust is estimated using a

linear programming approach to model residual GPS velocities. We find that older survey data can be used to investigate transient deformation behavior, if the displacements are sufficiently large and the measurements sampled often enough to separate steady state motions from transient displacements. However, the spatial distribution of transient slip before the onset of continuous GPS measurements is poorly constrained by the spatial and temporal sampling of survey GPS measurements in Guerrero.

[60] GPS measurements indicate that, at better than 95% confidence, motion reversed direction from the steady state velocity at sites ACAP, SANM, AYUT and UNIO between the 1995.7 and 1996.3 epochs of measurement. These motions are consistent with transient thrust slip just downdip of the seismogenic zone (Figure 8). However, given the sampling and uncertainties, the distribution of slip is unconstrained at the 95% confidence level. Moment release during the 1995–1996 event was equivalent to a $M_w = 7.1 + 1.3/-1.0$ earthquake, at 95% confidence. The temporal and spatial association of the 1995–1996 deformation and the Copala earthquake suggests postseismic slip downdip of the seismogenic zone, similar to that observed, e.g., following the 1997 Kronotskoë earthquake [Bürgmann *et al.*, 2001].

[61] We present here additional evidence for the 1998 transient slip event previously described by Lowry *et al.* [2001] from continuous data at CAYA, including corroborating displacements at survey sites and at the continuous GPS sites POSW and POPN on Popocatepetl volcano. The data provide a better constraint for modeling than for the 1995–1996 transient slip. Thrust slip is required at better than 95% confidence, and slip is limited to the region west of Acapulco, but the northern, southern and western boundaries of slip are indeterminate from the data. Moment release during the 1998 slip event was equivalent to a $M_w = 7.1 + 0.4/-0.1$ earthquake. The best fit model indicates slip within the region where seismogenic strain release would be expected, but this model is statistically indistinguishable from other models that place slip entirely downdip of the seismogenic zone. No large seismic events occurred on the Cocos-North America plate boundary that might reasonably have triggered the 1998 slip.

[62] The steady state slip model is used primarily to interpolate steady state velocities from well-sampled sites to poorly sampled sites, so that these velocities can be subtracted from the survey data yielding better spatial sampling of transient motions. The coupling model is sensitive to uncertainties in the estimates of GPS velocities and should be viewed with some skepticism in poorly sampled regions. However, the coupling model suggests that the shallow seismogenic portion of the Guerrero megathrust is at least partially locked, and that deeper portions of the plate interface are frictionally coupled as well. Deeper coupling is expected if transient slip is releasing interevent strain accumulated in regions of transitional frictional properties. The shallower coupling accumulates strain that may eventually be released in an earthquake.

[63] Although we have demonstrated here that survey data can be used to describe transient deformation, clearly continuous measurement is preferable. We have recently installed continuous GPS instrumentation at six sites in Guerrero and neighboring Oaxaca in a joint UNAM-CU project, and another six are under construction. Coupled

with the eight continuous GPS sites used in this study, these will permit us to characterize the spatial and temporal evolution of future transient events in much greater detail than was possible for these early events.

[64] **Acknowledgments.** The GPS surveys in 1992, 1995 and 1996 were supported by CONACYT grant 1089-T9201. The GPS surveys in 1998 and 2000 were supported by CONACYT grant G25842-T and NSF grant EAR-9725712 with technical assistance from UNAVCO. Additional support for CU investigators was provided by NSF grant EAR-0125618. All maintenance, data acquisition, and technical service of the continuous GPS stations was provided by Jose Antonio Santiago with the financial support of IN102697 (PAPIIT), 4960-T and G25842-T (CONACYT). V.K. and Roger Bilham installed the CAYA GPS receiver, which was purchased with NSF major equipment funding. The GPS survey and continuous data are archived at UNAVCO Inc. (<http://www.unavco.org>). We thank the Servicio Sismológico Nacional and particularly Casiano Jiménez Cruz, Javier Pacheco and Shri Krishna Singh for their efforts in collecting and processing most of the seismic data used in this research. Yehuda Bock provided a receiver for use at YAIG. NASA, Tim Dixon, and Enrique Cabral supported the installations of POSW and POPN. K.L. thanks UNAM for hosting her stay as a visiting scientist in November, 2000. Precise orbits from the International GPS Service and the Jet Propulsion Laboratory are gratefully acknowledged. An earlier draft of this paper was improved by critical readings by Nancy King, Greg Anderson, John Beavan, an anonymous reviewer, and an anonymous associate editor. The paper was also improved by constructive comments of referees Paul Segall, Christophe Vigny and associate editor Helene Lyon-Caen. Some of the figures were generated using the Generic Mapping Tools package [Wessel and Smith, 1998].

References

- Altamimi, Z., P. Sillard, and C. Boucher (2002), ITRF2000: A new release of the International Terrestrial Reference Frame for Earth science applications, *J. Geophys. Res.*, *107*(B10), 2214, doi:10.1029/2001JB000561.
- Anderson, J. G., S. K. Singh, J. M. Espindola, and J. Yamamoto (1989), Seismic strain release in the Mexican subduction thrust, *Phys. Earth Planet. Inter.*, *58*, 307–322.
- Beck, J. V., and K. J. Arnold (1977), *Parameter Estimation in Engineering and Science*, John Wiley, Hoboken, N. J.
- Beutler, G., I. I. Mueller, and R. E. Neilan (1994), The International GPS Service for Geodynamics (IGS): Development and start of official service on January 1, 1994, *Bull. Geod.*, *68*, 39–70.
- Blewitt, G. (1989), Carrier phase ambiguity resolution for the Global Positioning System applied to geodetic baselines up to 2000 km, *J. Geophys. Res.*, *94*, 10,187–10,203.
- Burbach, G., C. Frolich, W. Pennington, and T. Matumoto (1984), Seismicity and tectonics of the subducted Cocos plate, *J. Geophys. Res.*, *89*, 7719–7735.
- Bürgmann, R., M. G. Kogan, V. E. Levin, C. H. Scholz, R. W. King, and G. M. Steblov (2001), Rapid aseismic moment release following the 5 December, 1997 Kronotsky, Kamchatka, earthquake, *Geophys. Res. Lett.*, *28*, 1331–1334.
- Cocco, M., J. Pacheco, S. K. Singh, and F. Courboulex (1997), The Zihuatanejo, Mexico, earthquake of 1994 December 10 ($M = 6.6$): Source characteristics and tectonic implications, *Geophys. J. Int.*, *131*, 135–145.
- Courboulex, F., M. A. Santoyo, J. F. Pacheco, and S. Singh (1997), The 14 September 1995 ($M = 7.3$) Copala, Mexico, earthquake: A source study using teleseismic, regional, and local data, *Bull. Seismol. Soc. Am.*, *87*, 999–1010.
- Darby, D., and J. Beavan (2001), Evidence from GPS measurements for contemporary interplate coupling on the southern Hikurangi subduction thrust and for partitioning of strain in the upper plate, *J. Geophys. Res.*, *106*, 30,881–30,891.
- DeMets, C., R. G. Gordon, D. F. Argus, and S. Stein (1994), Effect of recent revisions to the geomagnetic reversal time scale on estimates of current plate motions, *Geophys. Res. Lett.*, *21*, 2191–2194.
- Dragert, H., K. Wang, and T. S. James (2001), A silent slip event on the deeper Cascadia subduction interface, *Science*, *292*, 1525–1528.
- Dziewonski, A. M., G. Ekstrom, and N. N. Maternovskaya (2001), Centroid-moment tensor solutions for July–September 2000, *Phys. Earth Planet. Inter.*, *124*, 9–23.
- Flück, P., R. D. Hyndman, and K. Wang (1997), Three-dimensional dislocation model for great earthquakes of the Cascadia subduction zone, *J. Geophys. Res.*, *102*, 20,539–20,550.
- Freymueller, J., and J. Beavan (1999), Absence of strain accumulation in the western Shumagin segment of the Alaska subduction zone, *Geophys. Res. Lett.*, *26*, 3233–3236.
- Haines, B. J., D. Dong, S. D. Desai, and S. Nerem (2001), Bringing tide gauges into the terrestrial reference frame: GPS results to support calibration of the emerging altimetric sea-level record, *Eos Trans. AGU*, *82*(47), Fall Meet. Suppl., Abstract G31D-08.
- Hirose, H., K. Hirahara, F. Kimata, N. Fujii, and S. Miyazaki (1999), A slow thrust slip event following the two 1996 Hyuganada earthquakes beneath the Bungo Channel, southwest Japan, *Geophys. Res. Lett.*, *26*, 3237–3240.
- Hutton, W., C. DeMets, O. Sánchez, G. Suárez, and J. Stock (2001), Slip dynamics during and after the 9 October 1995 $M_w = 8.0$ Colima-Jalisco earthquake, Mexico, *Geophys. J. Int.*, *146*, 637–658.
- Kostoglodov, V., W. Bandy, J. Domínguez, and M. Mena (1996), Gravity and seismicity over the Guerrero seismic gap, Mexico, *Geophys. Res. Lett.*, *23*, 3385–3388.
- Kostoglodov, V., S. K. Singh, J. A. Santiago, S. I. Franco, K. M. Larson, A. R. Lowry, and R. Bilham (2003), A large silent earthquake in the Guerrero seismic gap, Mexico, *Geophys. Res. Lett.*, *30*(15), 1807, doi:10.1029/2003GL017219.
- Lapusta, N., J. R. Rice, Y. Ben-Zion, and G. Zheng (2000), Elastodynamic analysis for slow tectonic loading with spontaneous rupture episodes on faults with rate- and state-dependent friction, *J. Geophys. Res.*, *105*, 23,765–23,789.
- Larson, K., J. Freymueller, and S. Philipsen (1997), Global plate velocities from the Global Positioning System, *J. Geophys. Res.*, *102*, 8892–9961.
- Larson, K. M., P. Cervelli, M. Lisowski, A. Miklius, P. Segall, and S. Owen (2001), Volcano monitoring using GPS: 1. Filtering strategies, *J. Geophys. Res.*, *106*, 19,453–19,464.
- Lichten, S., and J. Border (1987), Strategies for high precision GPS orbit determination, *J. Geophys. Res.*, *92*, 12,751–12,762.
- Lisowski, M., J. C. Savage, W. H. Prescott, and W. K. Gross (1988), Absence of strain accumulation in the Shumagin seismic gap, Alaska, 1980–1987, *J. Geophys. Res.*, *93*, 7909–7922.
- Lowry, A. R., K. M. Larson, V. Kostoglodov, and R. G. Bilham (2001), Transient slip on the subduction interface in Guerrero, southern Mexico, *Geophys. Res. Lett.*, *28*, 7909–7922.
- Marquez-Azua, B., and C. DeMets (2003), Crustal velocity field of Mexico from continuous GPS measurements, 1993 to June 2001: Implications for the neotectonics of Mexico, *J. Geophys. Res.*, *108*(B9), 2450, doi:10.1029/2002JB002241.
- Mazzotti, S., X. L. Pichon, P. Henry, and S. Miyazaki (2000), Full inter-seismic locking of the Nankai and Japan-west Kurile subduction zones: An analysis of uniform elastic strain accumulation in Japan constrained by permanent GPS, *J. Geophys. Res.*, *105*, 13,159–13,177.
- Menke, W. (1984), *Geophysical Data Analysis: Discrete Inverse Theory*, Academic, San Diego, Calif.
- Nishenko, S. P., and S. Singh (1987), Conditional probabilities for the recurrence of large and great interplate earthquakes along the Mexican subduction zone, *Bull. Seismol. Soc. Am.*, *77*, 2095–2114.
- Okada, Y. (1985), Surface deformation due to shear and tensile faults in a half-space, *Bull. Seismol. Soc. Am.*, *75*, 1135–1154.
- Ortiz, M., S. K. Singh, V. Kostoglodov, and J. Pacheco (2000), Source areas of the Acapulco-San Marcos, Mexico earthquakes of 1962 ($M_w = 7.1$, 7.0) and 1957 ($M_w = 7.7$), as constrained by tsunami and uplift records, *Geophys. Res. Lett.*, *27*, 337–348.
- Owen, S., G. Anderson, D. C. Agnew, H. Johnson, K. Hurst, R. Reilinger, Z. K. Shen, J. Svarc, and T. Baker (2002), Early postseismic deformation from the 16 October 1999 M_w 7.1 Hector Mine, California, earthquake as measured by survey-mode GPS, *Bull. Seismol. Soc. Am.*, *92*, 1423–1432.
- Ozawa, S., M. Murakami, and T. Tada (2001), Time-dependent inversion study of the slow thrust event in the Nankai trough subduction zone, *J. Geophys. Res.*, *106*, 787–802.
- Pacheco, J., L. R. Sykes, and C. H. Scholz (1993), Nature of seismic coupling along simple plate boundaries of the subduction type, *J. Geophys. Res.*, *98*, 14,133–14,159.
- Pardo, M., and G. Suárez (1995), Shape of the subducted Rivera and Cocos plates in southern Mexico: Seismic and tectonic implications, *J. Geophys. Res.*, *100*, 12,357–12,373.
- Press, W. H., B. P. Flannery, S. A. Teukolsky, and W. T. Vetterling (1992), *Numerical Recipes in FORTRAN: The Art of Scientific Computing*, Cambridge Univ. Press, New York.
- Sagiya, T. (1999), Interplate coupling in the Tokai district, central Japan, deduced from continuous GPS data, *Geophys. Res. Lett.*, *26*, 2315–2318.
- Sato, R. (1979), Theoretical basis on relationships between focal parameters and earthquake magnitude, *J. Phys. Earth*, *27*, 353–372.
- Savage, J. C. (1983), A dislocation model of strain accumulation and release at a subduction zone, *J. Geophys. Res.*, *88*, 4984–4996.
- Savage, J. C., J. L. Svarc, W. H. Prescott, and W. K. Gross (1998), Deformation across the rupture zone of the 1964 Alaska earthquake 1993–1997, *J. Geophys. Res.*, *103*, 21,275–21,283.

- Segall, P., R. Bürgmann, and M. Matthews (2000), Time-dependent triggered afterslip following the 1989 Loma Prieta earthquake, *J. Geophys. Res.*, *105*, 5615–5634.
- Singh, S. K., and F. Mortera (1991), Source time functions of large Mexican subduction earthquakes, morphology of the Benioff zone, age of the plate, and their tectonic implications, *J. Geophys. Res.*, *96*, 21,487–21,502.
- Singh, S. K., J. Pacheco, M. Ordaz, and V. Kostoglodov (2000), Source time function and duration of Mexican earthquakes, *Bull. Seismol. Soc. Am.*, *90*, 468–482.
- Suárez, G., and O. Sánchez (1995), Shallow depth of seismogenic coupling in southern Mexico: Implications for the maximum size of earthquakes in the subduction zone, *Phys. Earth Planet. Inter.*, *93*, 53–61.
- Suárez, G., T. Monfret, G. Wittlinger, and C. David (1990), Geometry of subduction and depth of the seismogenic zone in the Guerrero gap, Mexico, *Nature*, *345*, 336–338.
- Valdés-González, C., and D. A. Novelo-Casanova (1998), The western Guerrero, Mexico, seismogenic zone from the microseismicity associated to the 1979 Petatlan and 1985 Zihuatanejo earthquakes, *Tectonophysics*, *287*, 271–277.
- Wessel, P., and W. H. F. Smith (1998), New, improved version of Generic Mapping Tools released, *Eos Trans. AGU*, *79*, 579.
- Zumberge, J., M. Heflin, D. Jefferson, M. Watkins, and F. Webb (1997), Precise point positioning for the efficient and robust analysis of GPS data from large networks, *J. Geophys. Res.*, *102*, 5005–5018.
-
- K. Hudnut, U.S. Geological Survey, Pasadena, CA 91106, USA.
W. Hutton, Hutton Consulting, Seattle, WA, USA.
V. Kostoglodov, O. Sánchez, and G. Suárez, Instituto de Geofísica, National Autonomous University of Mexico, Mexico City, DF 04510, Mexico.
K. M. Larson, Department of Aerospace Engineering Sciences, University of Colorado, Boulder, CO 80309-0429, USA. (kristine.larson@colorado.edu)
A. R. Lowry, Department of Physics, University of Colorado, Boulder, CO 80309, USA.